A MODEL FOR ESTIMATING SPECTRAL PROPERTIES OF WATER FROM RGB IMAGES

Henryk Blasinski, John Breneman IV, Joyce Farrell

Department of Electrical Engineering
Stanford University
Stanford, CA, USA

ABSTRACT

This paper presents an underwater image formation model incorporating scatter and spectral absorption curves of pure water and three other particle classes; phytoplankton, non-algal particles and colored dissolved organic matter. We also describe an algorithm allowing to derive these depth dependent curves from a sequence of RGB images of a known target. Underwater images generated using the model closely resemble the experimental ones acquired in a variety of conditions. Similarly, the estimated absorption curves, and relative particle concentrations agree with common sense expectations.

Index Terms— Absorption spectrum, underwater imaging, image formation models, scatter, phytoplankton, non-algal particles, colored dissolved organic matter

1. INTRODUCTION

In the past few years inexpensive and ruggedized cameras have gained immense popularity. As a consequence users started to acquire images in harsh environments, traditionally requiring specialized and expensive equipment. Social media websites became inundated with images captured in the air, mud, and very often underwater. This last category of images has become especially popular, despite the inherent difficulties in acquiring high quality, sharp pictures with vivid colors.

The problem of color correction of underwater images is not unknown to the community. For example [1] provides an interesting overview of the recently developed methods. They range from relatively simple color balancing approaches to probabilistic modeling of color change phenomena. Despite well developed models [2] most of the algorithms operate in the RGB camera space and relatively little work is done in the spectral domain [3]. Even if such analyses are conducted, the spectral curves are used uniquely for color correction purposes [4].

The main focus of the paper is to present a mathematical model for spectral analysis of water properties, rather than a color correction algorithm in the RGB space. The benefit of such an approach is twofold. First, with spectral estimates in place, novel color correction algorithms can be implemented [5]. Second, these estimates can be used to analyze the chemical composition of water and detect presence or absence of certain classes of particles. The proposed model produces renderings of underwater images that are visually similar to experimentally acquired data. Predicted water composition, and consequently its spectral characteristics, is in agreement with common sense expectations, however a more rigorous validation still needs to be performed.

2. IMAGE FORMATION MODEL

Usually, image formation in air and across short distances is described with a simple linear model [6]. The model relates the irradiance at the sensor m with the illuminant $I_0(\lambda)$ and the scene reflectance $r(\lambda)$

$$m = g \int s(\lambda) r(\lambda) I_0(\lambda) d\lambda. \tag{1}$$

The constant g jointly represents a large number of camera settings that effectively influence the gain, for example: exposure duration, ISO sensitivity and the f-number. The function $s(\lambda)$ characterizes the spectral responsivity of the sensor and other elements on the optical path: the lens, the near-infrared filter and the color filter array.

The above model is much less appropriate for long distance imaging, or when images are acquired in other media, specifically underwater [3, 7]. Under these conditions image formation models distinguish between two types of light rays. Direct rays originate from a light source; are attenuated as they propagate through the medium, and after reflection from the target arrive at the sensor. Scattered rays on the other hand are reflected towards the camera directly by the medium and do not interact with the imaged object. An image formation model including both types of rays and, for computational convenience, discretizing the continuous integration into N wavebands, can be presented as

$$m = g\Delta\lambda \left(\sum_{i=1}^{N} s_i r_i I_{d,i} + \sum_{i=1}^{N} s_i I_{s,i} \right) \tag{2}$$

where $I_{d,i}$ and $I_{s,i}$ represent the direct and scattered illuminant components in the ith spectral channel respectively and $\Delta\lambda$ is the wavelength discretization step.

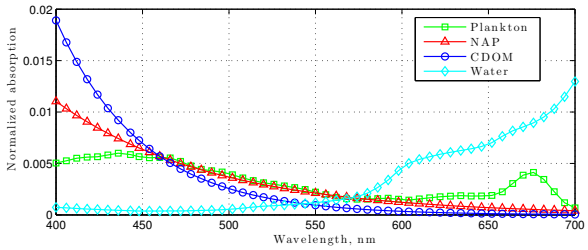

Fig. 1. Sample particle absorption curves normalized to unit surface area [10].

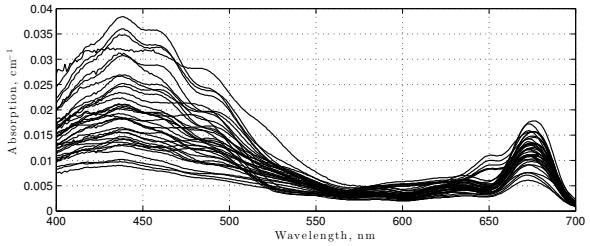

Fig. 2. Example absorption curves for a variety of plankton species [13].

2.1. Attenuation

Attenuation of light in a medium is governed by the well known Beer-Lambert's law [8]

$$I_{d,i} = I_{0,i} e^{-\alpha_{T,i} d} \tag{3}$$

where $I_{0,i}$ is the incident light intensity, $\alpha_{T,i}$ is the total spectral absorption coefficient of the medium and $I_{d,i}$ is the intensity of light after traveling distance d in the medium. In all cases the subscript i refers to the ith spectral band.

The literature on the physical properties of sea water describes four major classes of compounds contributing to the total absorption coefficient, α_T: phytoplankton, α_1, non-algal particles (NAP), α_2, colored dissolved organic matter (CDOM), α_3 and pure water, α_W [9]. Figure 1 presents sample absorption curves of individual components; their effect on the total absorption coefficient is additive, i.e

$$\alpha_T = \alpha_W + \sum_{k=1}^{3} \alpha_k \tag{4}$$

Figure 2 shows spectral absorption curves for different species of phytoplankton. Observe that all curves share common features, for example smoothness and peaks at about 450 and 675 nm. It is therefore fair to assume that these curves can be represented in a low dimensional space. Such a compact representation can be obtained using small number of linear basis functions

$$\alpha_T = \alpha_W + \sum_{k=1}^{3} B_k c_k \tag{5}$$

where, for the kth particle class, B_k represents a matrix of basis functions and c_k is the corresponding vector of basis function weights. The spectral absorption coefficient of pure water, α_W exhibits very little variability and therefore can be treated as a constant vector rather than a dependent variable [11, 12].

2.2. Scatter

Scatter involves complex interactions between the medium and the illuminant. A variety of scatter models have been proposed in the literature differing in their complexity and the number of free parameters [7, 8]. Since the scattered light does not interact with the scene, it will be assumed that the combined effect of $I_{s,i}$ and the camera responsivities s_i can be collapsed into a constant offset of an affine model, bs [14].

2.3. Simplified model

Incorporating the attenuation and scatter models into (2), the image formation model at depth d_j can be represented by

$$m_j = g\Delta\lambda \sum_{i=1}^{N} s_i r_i I_{0,i} e^{-\alpha_{T,i} d_j} + bs_j. \tag{6}$$

In the above equation $I_{0,i}$ represents the surface illuminant power in the ith spectral band. Similarly, $\alpha_{T,i}$ is the total absorption coefficient in the ith band and bs_j represents the offset due to scatter at depth j.

Rather than treating the entire water column of thickness d_j uniformly, it can be further subdivided into layers Δd_l thick, each characterized by its own set of absorption coefficients $\alpha_{T,l}$. Such a formulation allows for depth dependent variability of particle concentration. In this case the total attenuation at depth d_j can be expressed as

$$e^{-\alpha_T d_j} = e^{-\sum_{l=1}^{j} \alpha_{T,l} \Delta d_l} \qquad \Delta d_l = d_l - d_{l-1},\ d_0 = 0.$$

Incorporating this absorption coefficient decomposition in the image formation model (6) the response in the qth camera channel to a tth reflectance target at jth depth can be expressed as

$$m_{j,t,q} = g\Delta\lambda \sum_{i=1}^{N} s_{q,i} r_{t,i} I_{0,i} e^{-\sum_{l=1}^{j} \alpha_{l,i} \Delta d_l} + bs_{j,q} \tag{7}$$

$$\alpha_{l,i} = \alpha_{W,i} + \sum_{k=1}^{3} b_{k,i}^T c_{k,l}$$

where $b_{k,i}^T$ is the ith row of the basis function matrix for the kth particle class. The function (7) is not convex in all its parameters, i.e. surface illuminant I_0, absorption basis weights $c_{k,l}$ and the scatter term $bs_{j,q}$. However, given the surface illuminant I_0, $m_{j,t,q}$ becomes an affine function of $bs_{j,q}$ and a convex, non-increasing function of $c_{k,l}$'s.

3. MODEL ESTIMATION

In order to make the model estimation tractable it is necessary to know the spectrum of the surface illuminant $I_{0,i}$. As demonstrated in [15, 16] the spectra of natural illuminants can be compactly represented with a small number of basis functions and therefore can be reliably recovered from RGB images using a variety of computational techniques [17, 18].

Once the $I_{0,i}$'s are known, the estimation step consists in finding the spectral absorption weights $c_{k,l}$ as well as scatter offset terms bs_j using values captured by the camera $\hat{m}_{j,t,q}$. These weights can be found by solving the following minimization problem

$$\begin{array}{ll} \underset{c_{k,l},bs_j}{\text{minimize}} & \sum_{j,t,q} |\hat{m}_{j,t,q} - m_{j,t,q}|^{\gamma} + \delta \mathcal{R}(c_{k,l}) \\ \text{s.t.} & B_k c_{k,l} \geq 0 \qquad \forall_{k,l} \\ & b_j \geq 0 \qquad \forall_j \end{array} \tag{8}$$

where $\hat{m}_{j,t,q}$ represents the camera measurement of the tth target reflectance in the qth channel at the jth depth and $m_{j,t,q}$ are the values predicted by the model (7). The additional constraints arise from the non-negativity of the spectral absorption coefficients and scatter.

The function $\mathcal{R}(c_{k,l})$ introduces a depth dependent roughness penalty on the estimated coefficients. It is a weighted total variation penalty since it should account for samples taken at non-uniform depth intervals. An example function which heavily penalizes differences between coefficients at similar depths, and allows for large variations when the depth difference is large is

$$\mathcal{R}(c_{k,l}) = \sum_{k=1}^{3} \sum_{l=2}^{J} \frac{1}{(d_l - d_{l-1})^{\tau}} \left| c_{k,l} - c_{k,l-1} \right|, \tag{9}$$

with J being the total number of depth levels. As the parameter τ is increased the depth smoothness constraint becomes more and more local.

The fact that (7) is a smooth, convex, non-increasing function function of the parameters, makes the norm expression in the objective a quasiconvex function, provided $\gamma \geq 1$. Consequently the original problem (8) can be solved using convex optimization techniques.

The solution is found using an iterative algorithm and a first order Taylor series expansion of (7). When this expansion is substituted into (8) a norm of an affine function objective is obtained. The minimizer of this new objective function is then used as the approximation center for Taylor series expansion at the next iteration of the algorithm.

4. RESULTS

The image formation model was tested using a custom made rig consisting of an XRITE (Macbeth) color checker, a Canon SX260HS point and shoot camera in an underwater casing and a depth gauge. All the elements of the rig were attached to a rigid frame, fixing the camera to target distance to about 1m throughout the duration of the experiment. The color target was encased in polycarbonate to protect against the sea water. The original camera's firmware was replaced with CHDK[1], which gives users access to raw image data.

The data was acquired in the vicinity of Stanford's Hopkins Marine Station in the waters of Monterey Bay in California, USA. During each acquisition the camera was set in the time lapse photography mode and the rig was slowly lowered to the depth of about 20 meters. The camera operated in the aperture priority configuration, the firmware dynamically controlled the exposure duration and the ISO to account for the varying lighting. For further analysis two data sets were selected. One set containing 24 images was collected in very murky water, typical to that area. The second dive was conducted in exceptionally clear water and produced 13 images. Pixels from every patch were manually segmented to avoid reflections and water bubbles. For a given patch, at a given depth all segmented pixels were then averaged, producing a single triplet of values corresponding to camera red, green and blue channel responses.

4.1. Model accuracy

The correctness of the proposed model was evaluated by analyzing the relative error between the modeled response at optimal parameter values and the value acquired by the camera. The relative error approach allows to disregard the decrease of light intensity with depth and simultaneously analyze the data acquired at different depths. The average relative prediction errors are 18% and 15% for murky and clear water respectively. These values are comparable to the errors in the surface illuminant estimation with a linear model and three basis functions (20% and 10% respectively). Despite the relative error values, the measured and predicted images are visually identical. Figure 3 presents pairs of images for the two dives acquired at approximately 10 meters. The visual results are complemented in Fig. 4 by a scatter plot of modeled vs. acquired camera responses for these two image pairs.

4.2. Absorption and scatter

The algorithm for basis function weights computation was implemented in MATLAB and used the CVX convex optimization toolbox [19]. The objective function used $\gamma = 1$ and $\tau = 2$, these settings reduce the sensitivity for outliers and make the smoothness constraint more local. Finally the tradeoff parameter δ was set so that at the optimal point the roughness and model had about equal contributions to the objective. The iterative algorithm typically converged within five iterations. The plankton basis functions were derived from the numerical data presented in [9, 13, 20] using principal

[1] Canon Hack Development Kit, http://www.chdk.wikia.com

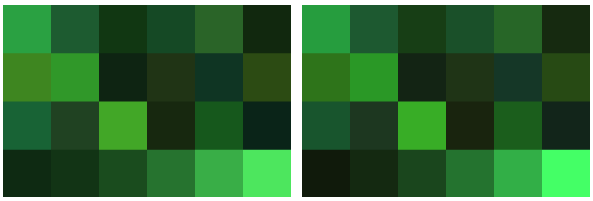

(a) Murky, captured (b) Murky, modeled

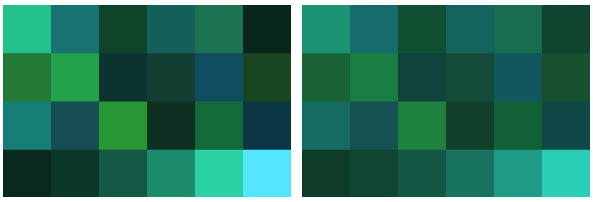

(c) Clear, captured (d) Clear, modeled

Fig. 3. Murky and clear water images at approximately 10 meters (best viewed in color).

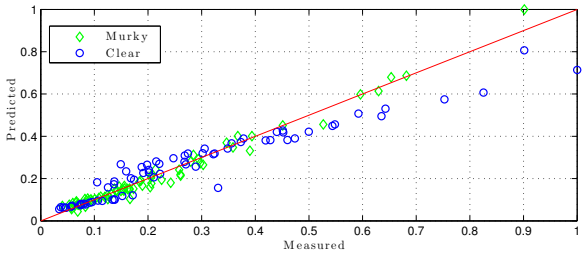

Fig. 4. Prediction scatter plot for data presented in Fig. 3

component analysis (PCA). Only two bases had their corresponding eigenvalues significantly larger than the remaining ones. The absorbance functions for non-algal particles and colored dissolved organic matter is usually modeled as exponentials with varying rates of decay [20]. For this reason both NAP and CDOM bases consisted of a single vector only. In total, at each depth four spectral parameters and three scatter parameters needed to be estimated.

Figure 5 shows examples of estimated absorption spectra for the two dives at about 10 meters. As expected, the murky water with highly greenish tint is quite rich in particle matter that strongly attenuates short wavelengths. On the other hand the clear water appears to have little particles as most of the absorption is attributed to pure water.

While the absorption curve of each of the particle class is highly correlated with its concentration, it is hard to determine its exact value if more than a single basis function is used. We propose to use a relative metric $\mathcal{M}$ to indicate how much each of the particle class contributes to the total absorption at a particular depth. This metric is the ratio between the area under the absorption curve of particle k divided by the area

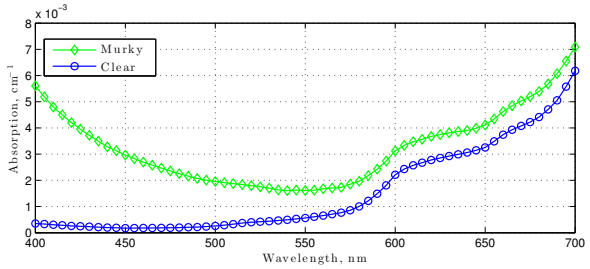

Fig. 5. Total absorption spectra at approx. 10 meters.

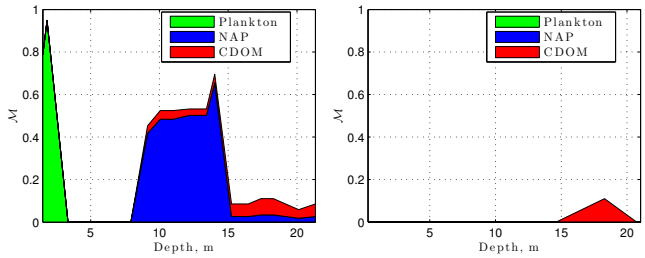

(a) Murky water (b) Clear water

Fig. 6. Water composition depth profiles, aera charts of relative particle contribution to total absorption.

under the total absorption curve

$$\mathcal{M}_k(d_j) = \frac{\sum_{i=1}^{N} \alpha_{k,i}(d_j)}{\sum_{i=1}^{N} \alpha_{T,i}(d_j)}. \tag{10}$$

Figure 6 presents the depth profiles of the parameter $\mathcal{M}_k$ for the two dives. Results highly agree with common sense expectations. The data from the clear water dive show very little presence of particulate matter and the most absorption phenomena are attributed to water. Interesting results can be observed in the case of the murky data. The profiles show increased plankton concentration close to the surface.This results is consistent with the well-known fat that phytoplankton is primarily composed of chlorophyl, which in turn requires light for photosynthesis. At deeper layers, the attenuation seems to be primarily related to other matter.

5. CONCLUSIONS

This paper describes an algorithm that uses RGB images and a reference target to analyze the spectral properties of water. Estimated absorption curves can be used for color balancing algorithms or, as presented here, to determine the presence of a variety particles in water. Algorithmic predictions of the underwater RGB images agree with the acquired data, however quantitative analysis still needs to be performed. Similarly, the accuracy of the proposed method could be increased by incorporating a scatter model which is also related to presence or absence of components in water.

6. REFERENCES

[1] Raimondo Schettini and Silvia Corchs, "Underwater image processing: State of the art of restoration and image enhancement methods," *EURASIP Journal on Advances in Signal Processing*, vol. 2010, no. 1, pp. 746052, 2010.

[2] Curtis Mobley and Charles Mobley, *Light and water: Radiative transfer in natural waters*, vol. 592, Academic Press, 1994.

[3] John Chiang and Ying-Ching Chen, "Underwater image enhancement by wavelength compensation and dehazing," *IEEE Transactions on Image Processing*, vol. 21, no. 4, pp. 1756–1769, 2012.

[4] Julia Ahlen, David Sundgren, and Ewert Bengtsson, "Application of underwater hyperspectral data for color correction purposes," *Pattern Recognition and Image Analysis*, vol. 17, no. 1, pp. 170–173, 2007.

[5] John Breneman, Henryk Blasinski, and Joyce Farrell, "The color of water: using underwater photography to estimatewater quality," in *Proc. SPIE*, 2014, vol. 9023, pp. 90230R–90230R–11.

[6] Joyce Farrell, Peter Catrysse, and Brian Wandell, "Digital camera simulation," *Appl. Opt.*, vol. 51, no. 4, pp. A80–A90, Feb 2012.

[7] Srinivasa Narasimhan and Shree Nayar, "Vision and the atmosphere," *International Journal of Computer Vision*, vol. 48, no. 3, pp. 233–254, 2002.

[8] Matthieu Boffety, Frédéric Galland, and Anne-Gaëlle Allais, "Color image simulation for underwater optics," *Appl. Opt.*, vol. 51, no. 23, pp. 5633–5642, Aug 2012.

[9] Marcel Babin, Dariusz Stramski, Giovanni Ferrari, Herve Claustre, Annick Bricaud, Grigor Obolensky, and Nicolas Hoepffner, "Variations in the light absorption coefficients of phytoplankton, nonalgal particles, and dissolved organic matter in coastal waters around europe," *Journal of Geophysical Research: Oceans*, vol. 108, no. C7, pp. 2156–2202, 2003.

[10] Collin Roesler and Mary Perry, "In situ phytoplankton absorption, fluorescence emission, and particulate backscattering spectra determined from reflectance," *Journal of Geophysical Research: Oceans*, vol. 100, no. C7, pp. 13279–13294, 1995.

[11] George Hale and Marvin Querry, "Optical constants of water in the 200-nm to 200-μm wavelength region," *Appl. Opt.*, vol. 12, no. 3, pp. 555–563, Mar 1973.

[12] Raymond Smith and Karen Baker, "Optical properties of the clearest natural waters (200–800 nm)," *Appl. Opt.*, vol. 20, no. 2, pp. 177–184, Jan 1981.

[13] Tetsuichi Fujiki and Satoru Taguchi, "Variability in chlorophyll a specific absorption coefficient in marine phytoplankton as a function of cell size and irradiance," *Journal of Plankton Research*, vol. 24, no. 9, pp. 859–874, 2002.

[14] Graham Finlayson, Steven Hordley, and Ruixia Xu, "Convex programming colour constancy with a diagonal-offset model," in *IEEE International Conference on Image Processing ICIP*, Sept 2005, vol. 3, pp. III–948–51.

[15] Deane Judd, David Macadam, Gunter Wyszecki, H. W. Budde, H. R. Condit, S. T. Henderson, and J. L. Simonds, "Spectral distribution of typical daylight as a function of correlated color temperature," *J. Opt. Soc. Am.*, vol. 54, no. 8, pp. 1031–1040, Aug 1964.

[16] Jeffrey DiCarlo and Brian Wandell, "Spectral estimation theory: beyond linear but before bayesian," *J. Opt. Soc. Am. A*, vol. 20, no. 7, pp. 1261–1270, Jul 2003.

[17] David Marimont and Brian Wandell, "Linear models of surface and illuminant spectra," *J. Opt. Soc. Am.*, vol. 9, no. 11, pp. 1905–1913, Nov 1992.

[18] Manu Parmar, Steven Lansel, and Joyce Farrell, "An LED-based lighting system for acquiring multispectral scenes," in *Proc. SPIE*, 2012, vol. 8299, pp. 82990P–82990P–8.

[19] Michael Grant and Stephen Boyd, "CVX: Matlab software for disciplined convex programming, version 2.0 beta," http://cvxr.com/cvx, Sept. 2013.

[20] Annick Bricaud, Andr Morel, Marcel Babin, Karima Allali, and Herv Claustre, "Variations of light absorption by suspended particles with chlorophyll a concentration in oceanic (case 1) waters: Analysis and implications for bio-optical models," *Journal of Geophysical Research: Oceans*, vol. 103, no. C13, pp. 31033–31044, 1998.